Academic Journal of Science and Technology
ISSN: 2771-3032 | Vol. 6, No. 3, 2023

Comparison and Analysis of SOC Estimation Based on First-Order and Second-Order Thevenin Battery Models Based on EKF

Yue Xia

School of Electrical Engineering, Southwest Minzu University, Chengdu, China

Abstract: The accurate modeling and estimation of state-of-charge (SOC) of lithium-ion batteries are of great significance for their utilization efficiency, service life extension and battery management system (BMS) design. This paper aims to provide understanding and guidance for understanding and guidance on different battery models and their parameter selection by comparing and analyzing the performance differences of Extended Kalman Filter (EKF) algorithm based on the first-order Thevenin battery model and the second-order Thevenin battery model. The Battery module in Matlab/Simulink is used to simulate the HPPC (HybridPulse Power Characterization) test of real batteries, and the model is parameterically identified. By establishing Thevenin battery models of different orders and applying the EKF algorithm for SOC estimation, the differences in accuracy, robustness and computational complexity of the two models are compared and analyzed, and experimental verification is carried out under different working conditions.

Keywords: State of charge, Equivalent circuit model, Parameter identification, Extended Kalman filtering.

1. Introduction

Lithium-ion batteries are widely used energy storage devices in modern society, and their status information is essential for battery management, performance optimization and safety evaluation [1]. SOC as an important indicator to describe the battery charge and discharge state, for electric vehicles, renewable energy storage and other fields of great significance, for electric vehicles, in China, Tsinghua University, Tongji University, Beijing Institute of Technology and many other universities on the battery management system (Battery Management System, BMS) related research and development. As one of the core technologies of BMS, battery SOC estimation is also constantly improving the optimization model and algorithm to improve the estimation accuracy [2]. Battery SOC estimation faces challenges such as model complexity, system uncertainty, measurement error and computational overhead, and the selection of appropriate battery models and estimation algorithms has become a key issue in research [3].

At present, the equivalent circuit models of lithium-ion batteries mainly include Rint model [4], first-order Thevenin model [5][6], second-order Thevenin model [7], PNGV model [8], GNL model [9]. On the basis of previous research, the advantages and disadvantages of each model are summarized, as shown in Table 1.

Table 1. Comparison of common battery models

Model name	complexity	advantage	drawback	precision
Rint model	simple	Simple and many applications	Does not reflect battery dynamics	Low
First-order Thevenin model	Relatively simple	better to simulate battery dynamics	Changes in current collection are not taken into account The change in the open circuit voltage of the current circuit	Lower
Second-order Thevenin model	More complex	Very good simulation of battery dynamics	Not suitable in engineering applications	moderate
PNGV model	Simpler	better to simulate battery dynamics	The circuit embodied by the change in current collection The change error of the open-circuit voltage is large	moderate
GNL model	complex	can accurately reflect the battery dynamics and has high accuracy	The structure is complex and the parameters are difficult to find	Higher

For lithium-ion batteries, the SOC estimation method mainly focuses on the perspective of energy conservation, that is, the remaining capacity of the battery is considered to be the ratio of the immediate remaining capacity of the battery to the total capacity of the battery [10]. At present, the main research methods for battery SOC estimation at home and abroad mainly include ampere-hour integral method, table lookup method, model-based method, and data-driven method [11][12], as shown in Figure 1. Among them, the model-based equivalent circuit method is the mainstream method for estimating SOC, which estimates SOC by identifying parameters of the model and then using the Kalman filter algorithm to estimate the SOC, because the battery model has nonlinearity, Kalman filter is not suitable

for nonlinear problems [13], while extended Kalman filtering can solve nonlinear problems well [14]. Wei Meng [15] et al. used unscented Kalman filtering based on Gaussian regression process to estimate SOC, and Xia Lili [16] et al. used adaptive Kalman filtering to correct the noise, and compared with these two methods, EKF significantly reduces the complexity of the algorithm under the premise of ensuring accuracy. Youping Liao of Beijing Institute of Technology used Thevenin model to estimate the SOC of the battery by the extended Kalman filter (EKF) algorithm, and realized the offline simulation of SOC in Matlab [17]. As commonly used battery modeling methods, the first-order Thevenin battery model and the second-order Thevenin battery model have different accuracy and computational complexity, which are of great significance for their application in battery SOC estimation.

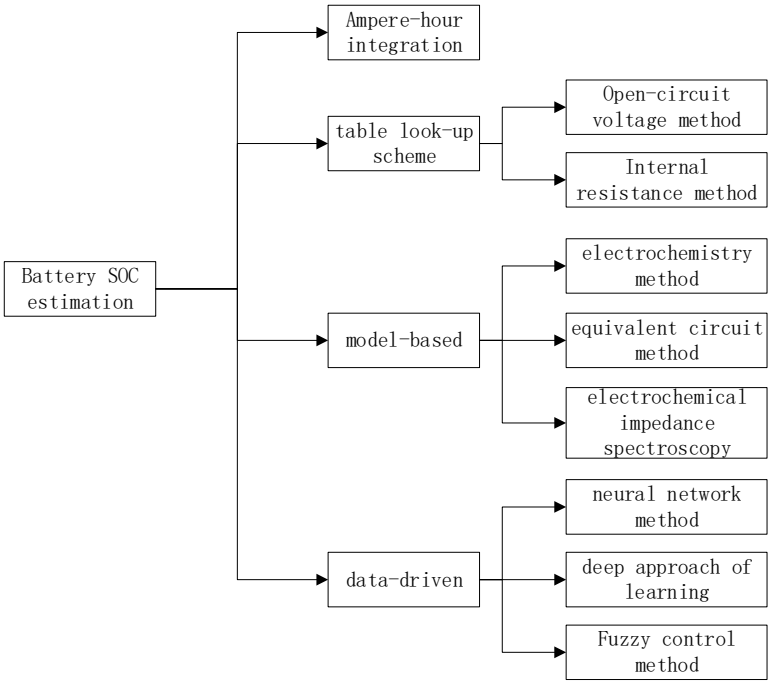

Figure 1. The main research methods of battery SOC at home and abroad

This paper aims to provide a reference for the selection and optimization of battery SOC estimation methods by comparing the performance difference of the EKF algorithm based on the first-order Thevenin battery model and the second-order Thevenin battery model. Through experimental verification and result analysis under different working conditions, we will compare the accuracy, robustness and computational complexity of the two models, and discuss their advantages, disadvantages and application scenarios, in order to provide useful guidance for the research and practical application of battery SOC estimation.

2. Battery Model and Parameter Identification

Compared with the complex chemical reactions inside the battery, the equivalent circuit model has been widely used in lithium-ion battery research based on its concise model and simple mathematical expression [7]. Establishing an equivalent circuit model is an effective method to realize battery SOC estimation based on the model method. Model accuracy is directly related to the estimation accuracy of SOC, and accurate modeling is conducive to accurately describing the external characteristics of the battery, and designing a more reliable battery state estimation algorithm to develop a better performance BMS [2]. At present, the Rint model [4], the first-order Thevenin model [5][6], the second-order Thevenin model [7], the PNGV model [8], and the GNL model [9]. This section briefly introduces the model characteristics of the first-order Thevenin model and the second-order Thevenin model.

2.1. First-order Thevenin model

The first-order Thevenin model introduces an RC loop based on the Rint model. The added RC loop can better simulate the slow change of battery terminal voltage, that is, reflect the battery polarization process, so the model can accurately reflect the charging and discharging process of the battery compared with the Rint model. The specific structure is shown in Figure 2.

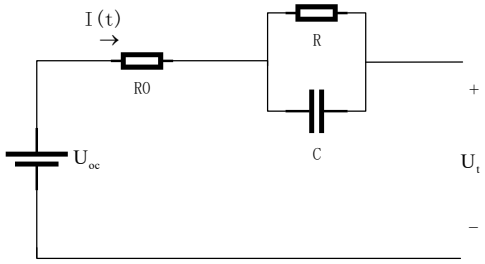

Figure 2. Equivalent circuit diagram of the first-order Thevenin battery model

According to Kirchhoff's laws we can get equations (1) and (2).

$$U_t = U_{ocv} - I(t) \cdot R_0 - U \tag{1}$$

$$\frac{dU}{dt} = \left(-\frac{1}{RC}\right) \cdot U + \frac{1}{C} \cdot I(t) \tag{2}$$

where U_t is the terminal voltage, U_ocv is the open-circuit

voltage, R_0 is the ohmic internal resistance, R is the polarized internal resistance, C is the polarized capacitor, and U is the voltage across the RC loop.

2.2. Second-order Thevenin model

The second-order Thevenin model introduces an RC loop based on the first-order Thevenin model. The two RC circuits of this model represent electrochemical polarization and concentration polarization during battery charging and discharging, respectively, and the simulation of internal dynamic polarization of the battery is more accurate. An RC loop of the first-order Thevenin model can only simulate the electrochemical polarization phenomenon during battery charging and discharging, although the dynamic characteristics of the battery are taken into account, but compared with the second-order Thevenin model, the effect of second-order Thevenin is theoretically better. The specific structure is shown in Figure 3.

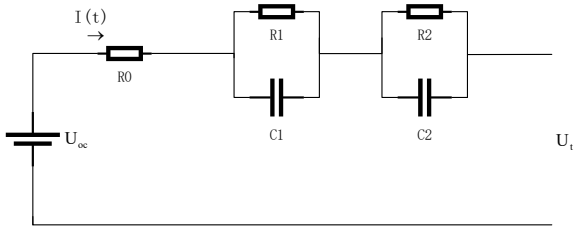

Figure 3. Second-order Thevenin battery model equivalent circuit diagram

According to Kirchhoff's law, equations (3), (4), (5) are obtained.

$$\frac{dU_1}{dt} = \left(-\frac{1}{R_1C_1}\right) \cdot U_1 + \frac{1}{C_1} \cdot I(t) \tag{3}$$

$$\frac{dU_2}{dt} = \left(-\frac{1}{R_2C_2}\right) \cdot U_2 + \frac{1}{C_2} \cdot I(t) \tag{4}$$

$$U_t = U_{oc} - I(t) \cdot R_0 - U_1 - U_2 \tag{5}$$

where U_t is the terminal voltage, U_ocv is the open-circuit voltage, the R_0 is the ohmic internal resistance, the R_1 is the load transfer impedance, the C_1 is the load transfer capacitance, the R_2 is the concentration impedance, the C_2 is the concentration capacitance, the U_1 is the voltage across the R_1 C_1 loop, and the U_2 is the voltage across the R_2 C_2 loop.

2.3. Identification and comparative analysis of battery model parameters

2.3.1. Parameter identification

The parameter identification results of the battery model directly determine whether the model can accurately simulate the real battery, that is, this link plays an important role in the battery modeling process. The parameter identification of the equivalent circuit model of lithium battery mainly has two modes: offline and online. The main purpose of this paper is to compare and analyze the SOC estimation of different orders of Thevenin battery models, so we chose simple offline identification. The offline identification of the equivalent circuit can be achieved by OCV-SOC curve fitting, and then the parameter identification of the battery model is carried out by pulse discharge, as shown in Figure 4 below.

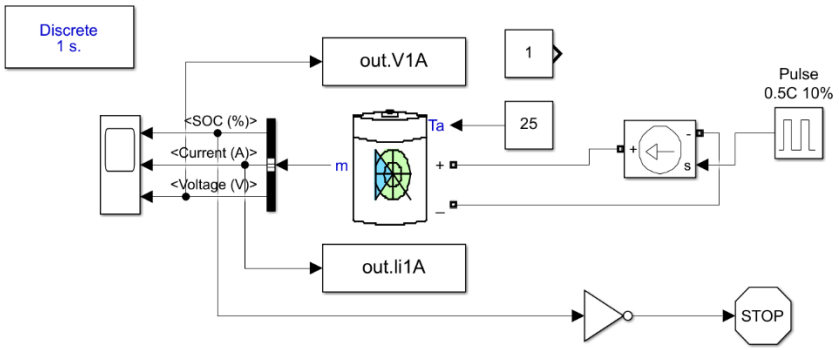

Figure 4. Simulation model of HPPC

This simulation simulates HPPC testing, where the battery is set with parameters that simulate the INR 18650-20R battery. The step is to perform test operations such as standing, discharging and charging of the battery in turn, perform an HPPC cycle test for each SOC point, record the open circuit voltage OCV value corresponding to each SOC value, and fit the OCV and SOC functions according to the recorded data, that is, equation (6). The seventh-order polynomial fit is obtained by using the Cftool toolbox in Matlab to obtain the curve relationship between OCV and SOC, that is, the soc-ocv curve. The fitting results are shown in Figure 5.

$$U_{ocv} = 14.63 \times SOC^7 - 58.42 \times SOC^6 + 97.99 \times SOC^5 - 89.8 \times SOC^4 + 48.93 \times SOC^3 - 16.16 \times SOC^2 + 3.552 \times SOC + 3.417 \tag{6}$$

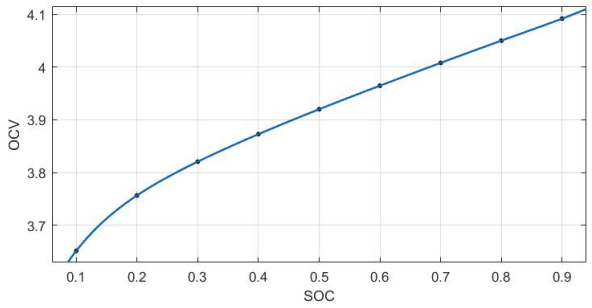

Figure 5. SOC-OCV fitting curve

As shown in Figure 6, the left figure is a simulated HPPC pulse discharge current and voltage, and the right figure is a local magnified view of the battery pulse discharge. It can be seen from the voltage curve of Figure 6 (left) that when the battery is suddenly powered off, the terminal voltage will

suddenly change, and the voltage will stabilize after a period of time, which is the voltage polarization phenomenon mentioned in the previous section. As shown in Figure 6 (right), the terminal voltage and current relationship of the stage discharge experiment, as can be seen from the figure, the voltage before point A is the shelving stage, when the battery begins to discharge, the terminal voltage instantly drops from point A to point B, point B to point C is the battery discharge stage, when the battery stops discharging, the terminal voltage rises instantaneously from point C to point D, point D to point E is the battery shelving stage, and the CE segment curve is the voltage polarization rebound curve.

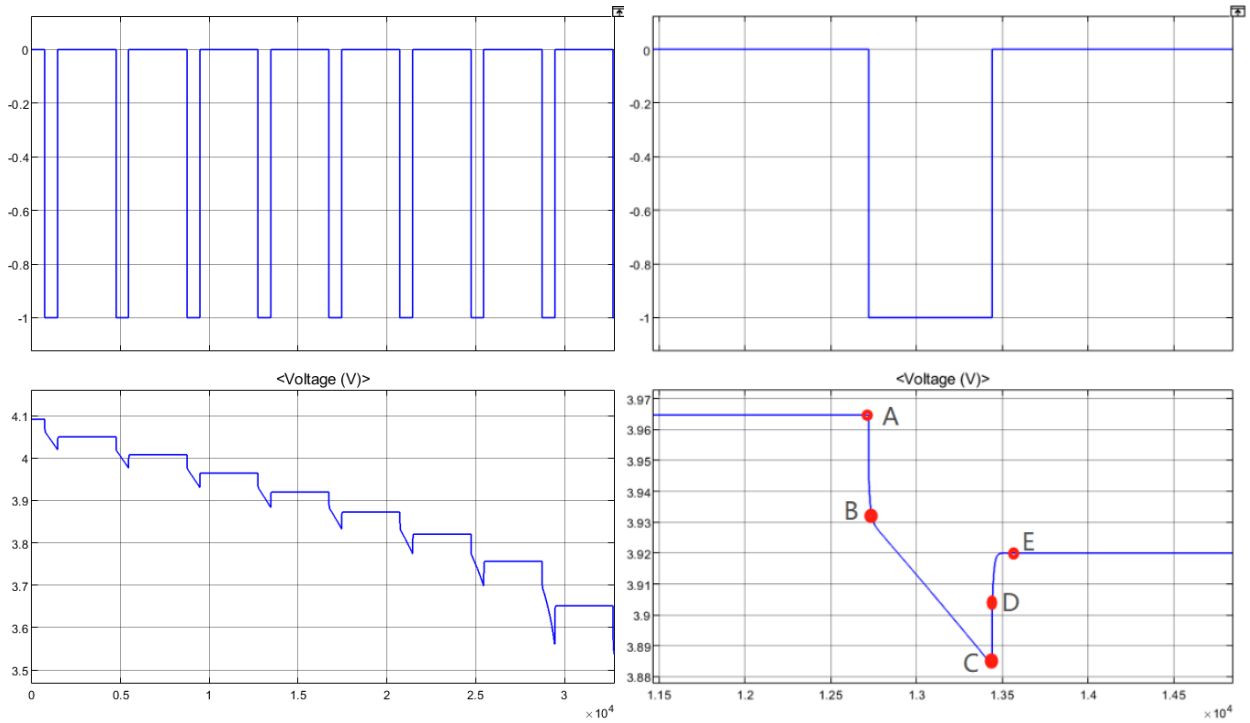

Figure 6. Battery pulse discharge current and voltage (left) pulse discharge partial magnification (right)

As shown in Figure 6 (right), when the battery at the beginning of discharge or the end of discharge, the battery terminal voltage will occur instantaneous mutation, this phenomenon is caused by ohmic internal resistance, because only the voltage on the ohmic internal resistance will change at the moment of discharge cut-off or start discharge, because there are two RC network loops in the model, the polarized capacitor can not discharge the polarization resistance in time, so the transition phenomenon cannot be caused by the polarized capacitance or resistance. In order to reduce the calculation error, two mutations at the beginning and end of the discharge are selected to calculate the ohmic internal resistance, as shown in Equation (7).

$$R_0 = \frac{(U_A - U_B) + (U_D - U_C)}{2I} \tag{7}$$

In the formula, U_A,U_B,U_C, and U_D are the terminal voltage values corresponding to points A, B, C, and D, and I is the discharge current of 0.5C (1A).

After the battery stage discharge stops, the response from point C to point E of the shelving time is regarded as a zero input response. The expressions corresponding to first-order Thevenin and second-order Thevenin are (8) and (9).

$$U(t) = U_{ocv} - IR_0 - U_1 e^{-\frac{t}{\tau}} - U_2 e^{-\frac{t}{\tau_2}} \tag{8}$$

$$U(t) = U_{ocv} - IR_0 - U_1 e^{-\frac{t}{\tau_1}} - U_2 e^{-\frac{t}{\tau_2}} \tag{9}$$

The second-order exponential fitting of the DE segment voltage in Figure 6 (right) is shown, and the fitting formulas of first-order Thevenin and second-order Thevenin are shown in (10) and (11), respectively, and the fitting results are obtained in Table 2 and Table 3, respectively.

$$y = y_0 - A \cdot e^{-\frac{t}{\tau}} \tag{10}$$

$$y = y_0 - A \cdot e^{-\frac{t}{\tau_1}} - B \cdot e^{-\frac{t}{\tau_1}} \tag{11}$$

Table 2. Parameter identification results of first-order Thevenin battery model

SOC (%)	R_0 (Ω)	R_c(Ω)	S (F)
90	4.09185	0.01997	0.02081
80	4.05012	0.01997	0.023
70	4.00789	0.01997	0.02618
60	3.96471	0.019965	0.0304
50	3.92003	0.019965	0.03624
40	3.87278	0.019965	0.04486
30	3.82056	0.019955	0.05886
20	3.75659	0.019935	0.08557
10	3.65152	0.01985	0.1567

Table 3. Parameter identification results of second-order Thevenin battery model

SOC (%)	R_0 (Ω)	R_1 (Ω)	R_2 (Ω)	C_1 (F)	C_2 (F)
90	0.01997	0.01031	0.00006337	970.902	16332.6495
80	0.01997	0.01149	0.000253	870.322	2075.4941
70	0.01997	0.01309	0.000594	763.9419	667.1717
S60	0.019965	0.0152	0.0005367	657.8947	792.6216
50	0.019965	0.01812	0.0005861	551.8764	637.4339
40	0.019965	0.02243	0.0001286	445.8315	6902.7994
30	0.019955	0.02944	0.000114	399.6739	3031.5789
20	0.019935	0.04281	0.0002695	233.5903	1312.8015
10	0.01985	0.07844	0.0001319	127.486	2056.1031

2.3.2. Comparative analysis of simulation results

According to the above offline identification results, the first-order Thevenin and second-order Thevenin equivalent circuit simulation models are built in Matlab/Simulink, and compared and analyzed with the battery module included in the simulink library. Figure 7 below.

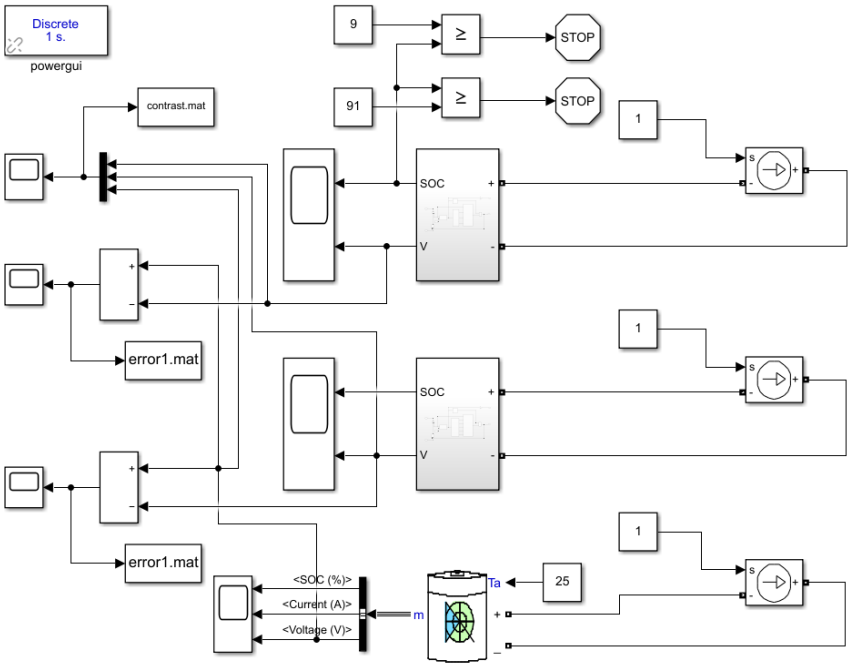

Figure 7. Comparison between the terminal voltage of the two models and the actual terminal voltage

Then the stage discharge condition is used for comparative analysis, see Figure 8-9.

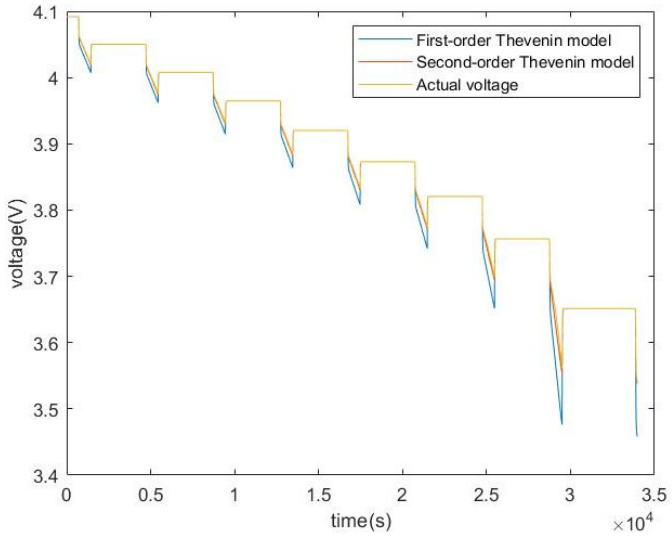

Figure 8. Comparison of the voltage of the two model terminals with the true value under the stage discharge

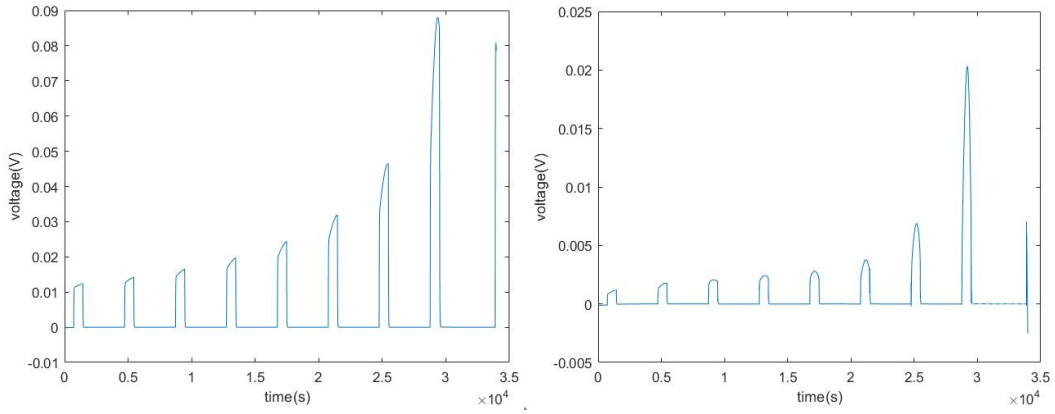

Figure 9. Next-order Thevenin error (left) and second-order Thevenin error (right) of stage discharge

It can be seen from Figure 9 that the mean absolute error (MAE) of the next-order Thevenin and second-order Thevenin at 0.5C constant current discharge is 0.0289 and 0.0041, respectively. From Figure 11, it can be seen that the average absolute errors of next-order Thevenin and second-order Thevenin in the stage discharge are 0.0265 and 0.0036, respectively. It can be seen that the terminal voltage accuracy of the second-order Thevenin model is higher than that of the first-order Thevenin model.

3. SOC Estimation of EKF

3.1. EKF

The standard Kalman filter (KF) method cannot be used in nonlinear systems due to its own characteristics, but mainly for linear systems, KF is discretized to obtain equations of state and observation equations, as shown in (12) below.

$$\begin{cases} x_{k+1} = Ax_k + Bu_k + w_k \\ y_k = Cx_k + Du_k + v_k \end{cases} \tag{12}$$

where，x_k is the n-dimensional state vector of the system、u_k is the system control input，y_k is the observation vector、A is the system transition matrix、B is the input matrix、C is the output matrix、D is a feed-forward matrix、w_k is process noise、v_k is observe noise。w_k and v_k are system noise and observation noise, respectively， the two are independent Gaussian white noises, $E[w_k] = 0$， $E\left[w_k\, w_j^T\right] = Q_k$， $E[v_k] = 0$， $E\left[v_k\, v_j^T\right] = R_k$.

When the system is linear, KF is mainly divided into two stages, the first stage is time update (prediction stage), that is, equation (13), (14), the second stage is measurement update (correction phase), that is, equation (15) ~ (17), the two stages have the following five recursive formulas, as follows.

Given initialized $\hat{x}_0$ and covariance matrix P_0

Status estimate time update

$$\hat{x}_{k/k-1} = A_{k-1}\hat{x}_{k-1} + B_{k-1}u_{k-1} \tag{13}$$

Error covariance prediction time update

$$P_{k/k-1} = A_{k-1}P_{k-1}A_{k-1}^T + Q_{k-1} \tag{14}$$

Kalman gain update

$$K_k = P_{k/k-1}C_k^T(C_kP_{k/k-1}C_k^T + R_k)^{-1} \tag{15}$$

Status estimation measurement update

$$\hat{x}_k = \hat{x}_{k/k-1} + K_k(y_k - C_k\hat{x}_{k/k-1} - D_ku_k) \tag{16}$$

Error covariance measurement update

$$P_k = P_{k/k-1} - K_kC_kP_{k/k-1} \tag{17}$$

thereinto，$\hat{x}_{k/k-1}$ is the predicted value of the current state at the moment，$\hat{x}_{k-1}$ is the optimal estimate for the previous moment，$\hat{x}_k$ is the optimal estimate of the system state variable at the next moment.

The battery system is a typical nonlinear system, especially the temperature and current changes of the battery will aggravate the nonlinearity of the battery system, so it is necessary to linearize the nonlinear system first. The advantage of the EKF method over the traditional KF method is that it can be applied to nonlinear systems. When the EKF method is applied to a nonlinear system, it is necessary to convert the nonlinear system, use the Taylor series to expand the system, retain the first-order derivative term and the constant term, ignore the advanced derivative term, so as to transform the nonlinear system into a linear system, and then use the KF method to complete the estimation of the system. Its system state space equation, such as Equation (18).

$$\begin{cases} x_k = f(x_k, u_k) + w_k \\ y_k = g(x_k, u_k) + v_k \end{cases} \tag{18}$$

where，$f(x_k, u_k)$ is a system nonlinear state transition function；$g(x_k, u_k)$ is a nonlinear observation function of the system；w_k and v_k are system noise and observation noise，the two are independent Gaussian white noises，$E[w_k] = 0$，$E\left[w_k\, w_j^T\right] = Q_k$，$E[v_k] = 0$，$E\left[v_k\, v_j^T\right] = R_k$。

For nonlinear functions $f(x_k, u_k)$ and $g(x_k, u_k)$ turn linearization，The Taylor series is expanded, ignoring the higher-order terms and retaining the first-order derivative term and constant term, thereby transforming the nonlinear function into a linear function, i.e. equations (19), (20).

$$f(x_k, u_k) \approx f(\hat{x}_k, u_k) + \left.\frac{\partial f(x_k, u_k)}{\partial x_k}\right|_{x_k=\hat{x}_k}(x_k - \hat{x}_k) \tag{19}$$

$$g(x_k, u_k) \approx g(\hat{x}_k, u_k) + \left.\frac{\partial g(x_k, u_k)}{\partial x_k}\right|_{x_k=\hat{x}_k}(x_k - \hat{x}_k) \tag{20}$$

Combined with KF linear system state space equations, cause $A_k = \frac{\partial f(x_k,u_k)}{\partial x_k}\Big|_{x_k=\hat{x}_k}$, $C_k = \frac{\partial g(x_k,u_k)}{\partial x_k}\Big|_{x_k=\hat{x}_k}$, The equations of state of a nonlinear system can be obtained from equations (18), (19), and (20), such as equation (21).

$$\begin{cases} x_{k+1} \approx A_k x_k + [f(\hat{x}_k,u_k) - A_k\hat{x}_k] + w_k \\ y_k \approx C_k x_k + [g(x_k,u_k) - C_k\hat{x}_k] + v_k \end{cases} \quad (21)$$

The following steps are the steps of KF, which leads to the ground inference process of the EKF algorithm.

3.2. SOC estimation of lithium-ion batteries based on EKF

Before using the EKF algorithm to perform SOC estimation for lithium titanate batteries, the main variables are selected. The current is the input of the entire system, the operating voltage of the battery is used as the observation variable, and the amount of time change under the action of the current is used as the state parameter.

Multiple state parameters are combined to form the state vector of the entire system [13]. Through the analysis of the first-order RC and second-order RC models, the voltage across the SOC and polarization resistor is selected as the state vector of the system, and the discrete state space model of the model is obtained. The mathematical formula for lithium-ion battery SOC is:

$$SOC = SOC_0 - \frac{1}{C_n}\int_0^t I(t)dt \quad (22)$$

thereinto, SOC_0 *is the SOC value at the moment* $t = 0$; SOC *is the SOC value at time* t; C_n is the rated capacity of the battery, unit is Ah. In this paper, the second-order RC model is used as an example.

Integrating the discretization of equations (3)(4)(5)(22) to obtain the equation of state (23) and the measurement equation (24) of the battery model.

Observation equation:

$$\begin{bmatrix} SOC_k \\ U_k^1 \\ U_k^2 \end{bmatrix} = \begin{bmatrix} 1 & 0 & 0 \\ 0 & e^{-T/\tau_1} & 0 \\ 0 & 0 & e^{-T/\tau_2} \end{bmatrix} \begin{bmatrix} SOC_{k-1} \\ U_{k-1}^1 \\ U_{k-1}^2 \end{bmatrix} + \begin{bmatrix} -T/C_n \\ R_1(1-e^{-T/\tau_1}) \\ R_2(1-e^{-T/\tau_2} \end{bmatrix} I_{k-1} + w_{k-1} \quad (23)$$

Measurement equation:

$$U_k = \begin{bmatrix} \frac{dU_{ocv}(SOC)}{dSOC} & -1 & -1 \end{bmatrix} \begin{bmatrix} SOC_k \\ U_k^1 \\ U_k^2 \end{bmatrix} - R_0 I_k + v_k \quad (24)$$

Thereinto, T is the experimental sampling period; U_k^1 and U_k^2 are the voltage values at k times C_1 and C_2, respectively; C_n is the battery capacity。 thereinto $x_k = \begin{bmatrix} SOC_k \\ U_k^1 \\ U_k^2 \end{bmatrix}$、$A_k = \begin{bmatrix} 1 & 0 & 0 \\ 0 & e^{-T/\tau_1} & 0 \\ 0 & 0 & e^{-T/\tau_2} \end{bmatrix}$、$B_k = \begin{bmatrix} -T/C_n \\ R_1(1-e^{-T/\tau_1}) \\ R_2(1-e^{-T/\tau_2} \end{bmatrix}$、$C_k = \begin{bmatrix} \frac{dU_{ocv}(SOC)}{dSOC} & -1 & -1 \end{bmatrix}$、$D_k = -R_0$, According to the ground pushing step of the KF method, SOC estimation can be completed according to equation (13)~(17).

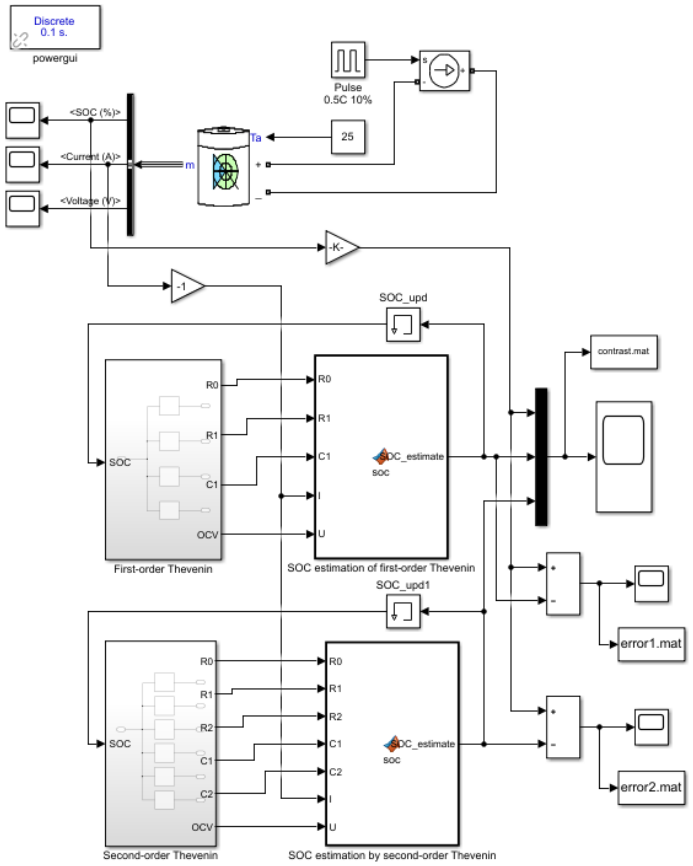

Figure 10. Comparison between the two models under stage discharge based on the estimated SOC of EKF and the actual

4. Simulation Verification and Comparative Analysis

Through the above data and analysis, the results of parameter identification are brought into the EKF algorithm, and then based on the steps of the above EKF algorithm, the program is written through the S-fuction module of simulink, where the estimation step is set to 0.1s, and the first-order Thevenin model and second-order Thevenin model based on the EKF algorithm are built in simulink to estimate SOC simulation and compared with the battery model included in simulink. In order to verify the accuracy of the algorithm, the stage discharge condition and the 0.5C constant current discharge condition are verified respectively, and Figure 12 is the simulation of the stage discharge condition.

At the same time, the SOC time change curve estimated by the EKF algorithm under the two models is obtained, namely Figure 13. The error of estimating SOC under the two models is shown in Figure 14, the error of first-order Thevenin estimating SOC on the left and the error of second-order Thevenin estimating SOC on the right. The error analysis of the two models is shown in Table 4.

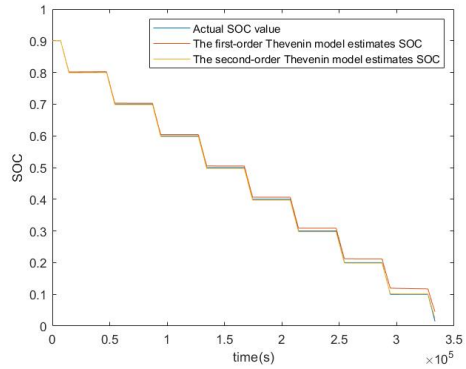

Figure 11. Comparison between the actual SOC value and the estimated SOC value of EKF based on the two models

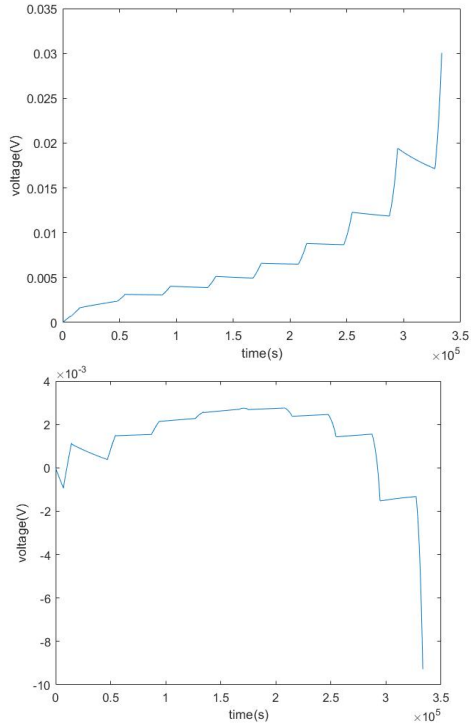

Figure 12. Based on first-order Thevenin error (left) and second-order Thevenin error (right)

Table 4. SOC estimation error analysis based on EKF algorithm for the two models

model	Mean squared error	Average absolute error(%)	Average absolute percentage error (%)
First-order Thevenin model	1.5816×10^{-4}	0.74	4.5
Second-order Thevenin model	$3.5735\times \mathbf{10^{-5}}$	0.19	0.79

It can be seen from Figure 14 and Table 4 that the use of EKF algorithm to estimate SOC under both models can achieve a good effect, under the same experimental conditions, the mean squared error, average absolute error and average absolute percentage error of EKF estimation SOC based on the second-order Thevenin model are smaller than the first-order Thevenin model, which shows that the error of the second-order Thevenin model is smaller and more accurate.

5. Conclusion

The accurate estimation of lithium-ion battery SOC can effectively improve the battery life and the safety and reliability of the battery use equipment. In this paper, the parameters of the first-order Thevenin model and the second-order Thevenin model are completed by using the Battery model in Simulink to simulate the battery for HPPC test. Based on the two models, a comparative experimental study on the accuracy of battery SOC estimation based on the EKF algorithm was completed. The results show that under the same experimental conditions, the EKF estimation method can improve the estimation accuracy of battery SOC. Compared with the first-order Thevenin model, the accuracy of EKF estimation SOC based on the second-order Thevenin model is significantly improved.

References

[1] Zhou, L., Cai, D., Yao, G., Yin, Z. (2019). Review of Key Technologies in Battery Management Systems. Battery, 49(04), 338-341. DOI: 10.19535/j.1001-1579.2019.04.018.

[2] Lu, L., Li, J., Hua, J., Ouyang, M. (2016). Key Technologies of Lithium-ion Battery Management System for Electric Vehicles. Science and Technology Review, 34(06), 39-51.

[3] Gao, M., Xu, H., Wu, M. (2021). Review of State-of-Charge Estimation Methods Based on Equivalent Circuit Models for Power Batteries. Journal of Electrical Engineering, 16(01), 90-102.

[4] Ramsey, D., German, R., et al. (2020). Comparison of Equivalent Circuit Battery Models for Energetic Studies on Electric Vehicles. In 17th IEEE Vehicle Power and Propulsion Conference (VPPC).

[5] Zhou, J., Hua, Y., Liu, K., Lan, H., Fan, C. (2019). Research on a High Precision Modeling Solution for Lithium-ion Batteries. Proceedings of the Chinese Society for Electrical Engineering, 39(21), 6394-6403. DOI: 10.13334/j.0258-8013.pcsee.182306.

[6] Milishchuk, R., Bogodorova, T. (2022). Thevenin-based Battery Model with Ageing Effects in Modelica. In 21st IEEE Mediterranean Electrotechnical Conference, 243-248.

[7] Ji, Y., Qiu, S., Li, G. (2020). Simulation of Lithium-ion Battery Second-order RC Equivalent Circuit Model Based on Variable Resistance and Capacitance. Journal of Central South University, 27(09), 2606-2613.

[8] Nejad, S., Gladwin, D.T., et al. (2016). A Systematic Review of Lumped-parameter Equivalent Circuit Models for Real-time Estimation of Lithium-ion Battery States. Journal of Power Sources, 316, 183-196.

[9] Yan, X., Guo, Y., Cui, Y., et al. (2018). Electric Vehicle Battery State of Charge Estimation based on GNL Model Adaptive Kalman Filter. Journal of Physics: Conference Series, 1087(5).

[10] Wang, Z., Li, R., Li, X. (2021). Lithium-ion Battery State of Charge Estimation based on Hybrid AUKF and HIFF. Battery, 51(04), 380-384. DOI: 10.19535/j.1001-1579.2021.04.013.

[11] Zhao, X., Li, M., Yu, Q., Ma, J., Wang, S. (2023). Overview of Lithium-ion Battery State Estimation for Electric Vehicle Power Systems. China Journal of Highway and Transport, 1-39. Retrieved from http://kns.cnki.net/kcms/detail/61.1313.U.20230420.1452.002.html

[12] Hua, Z., Li, J. (2013). Overview of State of Charge Estimation Methods for Electric Vehicle Power Batteries. Power Supply Technology, 37(09), 1686-1689.

[13] Guo, X., Hua, X., Fu, Z., et al. (2018). Kalman Filter State of Charge Estimation Based on Model Parameter Optimization. Journal of Electronic Measurement and Instrumentation, 32(8), 186-192.

[14] Xu, J., Liu, B.H., Wang, X.Y., et al. (2016). Computational Model of 18650 Lithium-ion Battery with Coupled Strain Rate and State of Charge Dependencies. Applied Energy, 172, 180-189.

[15] Wei, M., Li, J.B., Li, Z.Y., et al. (2020). State of Charge Estimation for Lithium-ion Batteries based on Gaussian Process Regression and Unscented Kalman Filter. Energy Storage Science and Technology, 9(4), 1206-1213.

[16] Xia, L., Wang, S.L., Yu, C.M., et al. (2021). Research on SOC Estimation Method of Ternary Lithium-ion Batteries based on AEKF Algorithm. Control Engineering, 28(4), 730-735.

[17] Liao, Y.P., Li, R., Lv, H., Zhang, F.J., Zhao, C.L. (2023). State of Charge Estimation of Lithium Titanate Battery based on Extended Kalman Filter. Power Supply Technology, 47(05), 639-643.